International Journal of Zoology and Applied Biosciences **ISSN: 2455-9571**
Volume 11, Issue 6, pp: 74-85, 2026
https://doi.org/10.55126/ijzab.2026.v11.i06.010 **http://www.ijzab.com**

Research Article

PHYTOCHEMICAL CHARACTERIZATION, ANTIOXIDANT AND ANTIMICROBIAL ACTIVITIES OF THE ETHANOLIC LEAF EXTRACT OF *ANDROGRAPHIS PANICULATA*: A GC-MS AND MOLECULAR DOCKING STUDY

[1]Sakthivel Mahalingam, [1]Thaila Srinivasan, [1]Vanmuhil Prabhu, [2]Raja Rajeshwari G, [3]Vijayan R, [3]Karthik Raja R, [4]Arjun Pandian, [5]Pennarasi Mohanraj, [1]*Ganesan Sivamani

[1]*PG & Research Department of Zoology, A.V.V.M. Sri Pushpam College (An Autonomous Institution Affiliated to Bharathidasan University), Poondi, Thanjavur 613503, Tamil Nadu, India.
[2]Saveetha Medical College and Hospital (SMCH), Saveetha Institute of Medical and Technical Sciences (SIMATS), Saveetha University, Chennai 602105, Tamil Nadu, India.
[3] Centre for Applied Research, Institute of Biotechnology, Saveetha School of Engineering (SSE), Saveetha Institute of Basic Medical Sciences (SIBMS), Saveetha Institute of Medical and Technical Sciences (SIMATS), Saveetha University, Chennai 602105, Tamil Nadu, India.
[4] Tissue Culture, Natural Products & Microbial Biotechnology Research Laboratory, Saveetha Institute of Basic Medical Sciences (SIBMS), Saveetha Institute of Medical and Technical Sciences (SIMATS), Saveetha University, Chennai 602105, Tamil Nadu, India.
[5] Arasi Bio Innovations, Biotechnology Research and Training Institute, 6/144, Vignesh Nivas, Madurai Veeran Nagar, Gundur, Tiruchirapalli-620007.

Article History: Received 27th August 2026; Accepted 25th October 2026; Published 1st November 2026

ABSTRACT

Andrographis paniculata (Burm.f.) Nees (Acanthaceae; green chiretta) is a medicinal herb widely used in Ayurvedic and other Asian traditional medicine for infectious and inflammatory conditions. To characterize the phytochemical profile of its ethanolic leaf extract, to evaluate its in vitro antioxidant and antimicrobial activities, and to make an exploratory in silico assessment of two GC-MS-detected constituents. Shade-dried leaves were extracted with ethanol (Soxhlet), screened for secondary metabolites and analysed by UV-Vis, FT-IR and GC-MS. Free-radical scavenging was measured by DPPH, ABTS and hydroxyl radical assays (100-500 µg/mL). Antimicrobial activity was determined by agar well diffusion against four bacteria and two *Candida* species. N-(tert-butyl)-2-benzoylbenzamide and butanedioic acid, 2-ethyl-2-(phenylthio)-, 1-ethyl ester (both tentative GC-MS library assignments) were docked (AutoDock; protocol not validated) against Smad3/Smad4 (PDB 1U7F) and Smurf2 (PDB 6FX4), regulators of TGF-β signalling. Alkaloids, phenols, flavonoids, tannins, steroids, saponins and terpenoids were detected. A UV maximum near 290 nm and FT-IR bands indicated phenolic/aromatic and carbonyl-containing groups. GC-MS resolved 15 peaks representing nine tentatively assigned compounds, four of which were classed as probable artefacts; the largest combined area (31.78%) was assigned to the butanedioate ester. At 500 µg/mL, scavenging was 79.13% (DPPH), 72.02% (ABTS) and 76.75% (hydroxyl radical) versus 21.32%, 17.32% and 17.28%, respectively, at 100 µg/mL; IC_{50} values were not determined. At 60 µL, the largest inhibition zones were against *Pseudomonas aeruginosa* (24 mm), *Salmonella typhimurium* (22 mm) and *Candida albicans* (21 mm). Unvalidated docking scores for N-(tert-butyl)-2-benzoylbenzamide were −8.05 (1U7F) and −7.73 kcal/mol (6FX4), versus −5.54 and −5.40 kcal/mol for the butanedioate ester. The extract showed radical-scavenging activity and inhibition zones against all six test organisms in vitro; these observations are preliminary. The GC-MS assignments are tentative and the docking results are hypothesis-generating only. Full concentration-response data (including IC_{50} determination), replicated measurements, minimum inhibitory concentrations, cytotoxicity testing, LC-MS confirmation of constituents and validated docking with molecular dynamics are needed. This work is relevant to SDG 3 (Good Health and Well-being).

*Corresponding Author: Ganesan Sivamani, PG & Research Department of Zoology, A.V.V.M. Sri Pushpam College (Autonomous), Poondi, Thanjavur 613503, Tamil Nadu, India Email: ganesanmolbio@gmail.com.

Keywords: *Andrographis paniculata,* GC-MS, Antioxidant, Antimicrobial, Molecular docking, Smad3.

INTRODUCTION

Andrographis paniculata (Acanthaceae), known as creat or green chiretta, is an annual herb native to India and Sri Lanka and cultivated across South and Southeast Asia. Its leaves, roots or whole plant are used traditionally for fever, respiratory and gastrointestinal infections, diabetes, hypertension, ulcers and skin disorders. The herb is included in World Health Organization monographs on medicinal plants (WHO, 2009), and critical reviews describe antibacterial, antiviral, anti-inflammatory and antineoplastic activities (Chen *et al*., 2023; Rahman and Husen, 2023; Rana *et al*., 2024). These effects are largely attributed to labdane diterpenoid lactones, chiefly andrographolide, together with flavonoids (Chen *et al*., 2023; Thai *et al*., 2025). Plant secondary metabolites (compounds not essential for growth but important for defence) such as phenols and flavonoids can neutralize reactive oxygen species (ROS), the unstable oxygen-derived molecules that damage lipids, proteins and DNA and contribute to diabetes, cancer, atherosclerosis and inflammatory disease (Chaudhary *et al*., 2023; Valgimigli, 2023; Ansari *et al*., 2025). The same metabolite classes can also disrupt microbial membranes and enzymes, which makes plant extracts a source of leads against bacteria and fungi, including those that cause foodborne and opportunistic infections (Anju *et al*., 2023; Salman *et al*., 2025).

Gas chromatography-mass spectrometry (GC-MS) separates volatile and semi-volatile compounds and identifies them from their mass spectra. Molecular docking is a computational method that predicts how a small molecule (ligand) orients and binds within a protein, and ranks it by estimated binding free energy (kcal/mol; more negative means stronger predicted binding). Smad3 and Smad4 are intracellular transducers of transforming growth factor-β (TGF-β) signalling, and Smurf2 is a HECT-type E3 ubiquitin ligase that tags Smad proteins for proteasomal degradation and so modulates the pathway (Lin *et al*., 2000). Dysregulated TGF-β/Smad signalling is implicated in fibrosis and tumour progression (Mekky *et al*., 2025), and natural products such as rhein and curcumin have been reported to act on Smad3 and Smurf2 respectively (Zheng *et al*., 2025; Xi *et al*., 2025). These proteins were therefore chosen as exploratory targets for GC-MS-detected constituents. The objectives of this study were to (i) screen and characterize the metabolite profile of the ethanolic leaf extract by phytochemical tests, UV-Vis, FT-IR and GC-MS; (ii) assess antioxidant activity by DPPH, ABTS and hydroxyl radical assays; (iii) assess antimicrobial activity against selected bacteria and *Candida* species; and (iv) explore in silico interactions of two detected compounds with Smad3/Smad4 and Smurf2.

MATERIALS AND METHODS

Plant material and extraction

Leaves of *A. paniculata* were collected, shade-dried and powdered. Twenty grams of powder in a filter-paper thimble was extracted with ethanol in a Soxhlet apparatus (continuous hot percolation of solvent through the sample), and the extract was concentrated by rotary evaporation (Arjun, 2011).

Qualitative phytochemical screening

Alkaloids, phenols, flavonoids, proteins, tannins, steroids, saponins and terpenoids were tested by standard colour or precipitation reactions (Sumathy *et al*., 2025). The tests used for the respective classes were Mayer/Wagner (alkaloids), ferric chloride (phenols), alkaline reagent (flavonoids), Biuret (proteins), gelatin (tannins), Liebermann-Burchard (steroids), froth test (saponins) and Salkowski (terpenoids).

UV-Vis spectroscopy

The extract was scanned from 200 to 800 nm on a PerkinElmer UV-Vis spectrophotometer (Sukirtha *et al*., 2025). UV-Vis detects chromophores, i.e. groups such as aromatic rings and conjugated double bonds that absorb light.

FT-IR spectroscopy

The extract was mixed with potassium bromide (KBr), pressed into a pellet and scanned from 4000 to 500 cm^{-1} on a Shimadzu 8400S spectrometer (Azhagu Madhavan and Arjun, 2025). Fourier-transform infrared (FT-IR) spectroscopy assigns functional groups from the wavenumbers at which bonds vibrate.

GC-MS analysis

Analysis used a PerkinElmer GC-MS system with an Elite-1 capillary column (100% dimethyl polysiloxane; 30 m × 0.25 mm ID, 0.25 µm film thickness). Helium was the carrier gas, with a split ratio of 10:1 and an injector at 250 °C. The oven was held at 110 °C for 2 min, raised at 10 °C/min to 220 °C, then at 5 °C/min to 280 °C. The ion source was at 280 °C, with electron-impact ionization at 70 eV and a scan range of 45-450 Da (0.5 s scan). Data were processed in TurboMass 5.0. A solvent (ethanol) blank was run under identical conditions. Compounds were tentatively assigned by comparing mass spectra with the NIST library and retention indices relative to n-alkanes (Arjun *et al*., 2017). NIST match factors and retention-index values are not reported here, and no authentic reference standards are described. Peaks that matched siloxanes (column or septum bleed) or reagent-type derivatives, and that appeared in the blank or were chemically implausible as plant metabolites, were classed as probable artefacts.

Molecular docking

Crystal structures of the Smad3/Smad4 complex (PDB 1U7F) and human Smurf2 (PDB 6FX4) were obtained from the RCSB Protein Data Bank. Water molecules and heteroatoms were removed in PyMOL (DeLano, 2002), and polar hydrogens and Gasteiger charges were added. Ligand structures were retrieved from PubChem, energy-minimized in GaussView 6.0 and saved in PDB format. Docking used AutoDock 4 (Morris *et al*., 2009); nine conformations were generated per ligand and the lowest-energy pose was retained. No validation of the docking protocol (for example, redocking of a native ligand with RMSD calculation) is reported, so the scores are treated as exploratory. Interactions were analysed in BIOVIA Discovery Studio (Sharma *et al*., 2021).

Antioxidant assays

All assays used extract concentrations of 100-500 µg/mL with ascorbic acid as the reference standard. Results are reported only for the lowest (100 µg/mL) and highest (500 µg/mL) concentrations; intermediate readings and the ascorbic acid reference values are not available in the present dataset. Percentage inhibition = $[(A_0 - A)/A_0] \times 100$, where A_0 is the control absorbance and A the sample absorbance. DPPH (2,2-diphenyl-1-picrylhydrazyl, a stable purple radical that turns yellow when it accepts a hydrogen atom or electron): the extract was mixed with methanolic DPPH, and absorbance was read at 517 nm (Sumathy *et al*., 2024; Brand-Williams *et al*., 1995). ABTS (2,2′-azino-bis(3-ethylbenzothiazoline-6-sulfonic acid), a blue-green radical cation, $ABTS^{+}$): decolourization was read at 734 nm (Re *et al*., 1999; Hariprasath *et al*., 2016). Hydroxyl radical (OH, the most reactive ROS; generated by $Fe^{3+}/EDTA/H_2O_2$ and detected by deoxyribose degradation): the mixture was incubated for 30 min at 80 °C and absorbance read at 532 nm (Halliwell *et al*., 1987; Azhagu Madhavan *et al*., 2024).

Antimicrobial assay

Activity was tested by agar well diffusion, in which extract diffuses from a well into seeded agar and a clear zone shows growth inhibition (Balouiri *et al*., 2016; Güler *et al*., 2023). Test organisms were *Micrococcus luteus* (Gram-positive), *Escherichia coli*, *Pseudomonas aeruginosa* and *Salmonella typhimurium* (Gram-negative), and *Candida albicans* and *Candida glabrata* (yeasts). Mueller-Hinton agar (11.4 g in 300 mL distilled water) was autoclaved at 115 °C (10 lb) for 30 min, and 20 mL was poured per plate. Plates were swabbed with each inoculum, and 8 mm wells were punched. Wells received 20, 40 or 60 µL of extract. Amoxicillin (bacteria) and fluconazole (yeasts) were positive controls and DMSO was the negative control. Plates were incubated at 37 °C for 24 h, and zone diameters (including the 8 mm well) were measured in mm with a ruler.

Statistical analysis

Antioxidant and antimicrobial results are reported as the individual measurements recorded (n = 1 per condition). No standard deviations were calculated and no inferential statistical tests were performed; accordingly, no statements of statistical significance are made.

RESULTS AND DISCUSSION

The ethanolic extract gave positive tests for alkaloids, phenols, flavonoids, tannins, steroids, saponins and terpenoids, and a negative test for proteins (Table 1). Phenols and flavonoids are associated with antioxidant and antimicrobial action, tannins with astringent and anti-inflammatory effects, saponins with membrane-disrupting antibacterial effects, and alkaloids with diverse pharmacological activity (Azhagu Madhavan *et al*., 2025). These associations are literature-based and were not individually tested here.

Table 1. Secondary metabolites in the ethanolic leaf extract of *A. paniculata* (+ present, − absent).

S. No.	Phytochemical class	Result
1	Alkaloids	+
2	Phenols	+
3	Flavonoids	+
4	Proteins	−
5	Tannins	+
6	Steroids	+
7	Saponins	+
8	Terpenoids	+

The spectrum showed an absorption maximum (λ_{max}) near 290 nm (Figure 1). Bands in this region arise from $\pi \rightarrow \pi^*$ electronic transitions (promotion of an electron from a bonding π to an antibonding π^* orbital) in aromatic rings and conjugated systems, and are typical of phenolic compounds and flavonoids. This is consistent with the positive phenol and flavonoid tests but is not by itself compound-specific.

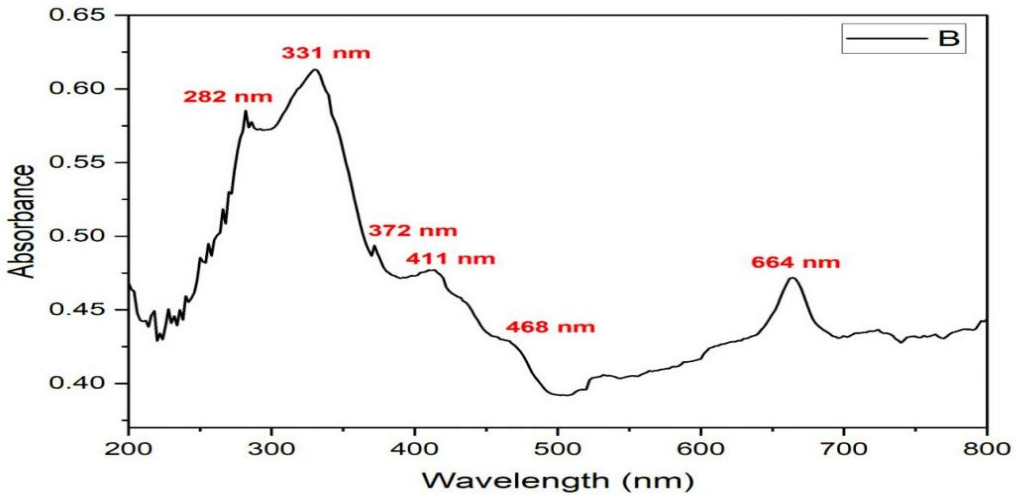


Figure 1. UV-Vis absorption spectrum of the ethanolic leaf extract of *A. paniculata*; $\lambda_{max} \approx 290$ nm.

Bands were observed between 3290 and 776 cm^{-1} (Figure 2, Table 2). The broad band at 3290 cm^{-1} indicates hydrogen-bonded O-H (alcohols or phenols), and the 2920/2843 cm^{-1} pair indicates aliphatic CH_2 stretches. The band at 1732 cm^{-1} indicates a carbonyl, most consistent with an ester; 1628 and 1600 cm^{-1} indicate C=C of conjugated alkenes and aromatic rings; and bands at 1320, 1244 and 1027 cm^{-1} indicate C-O and C-O-C of phenols, ethers and alcohols or glycosides. Out-of-plane aromatic C-H bending appears at 894 and 776 cm^{-1}. A previous FT-IR study of *A. paniculata* leaves similarly reported O-H near 3323 cm^{-1} and alkene C=C near 1645 cm^{-1} (Maria *et al*., 2018). FT-IR identifies functional groups, not individual compounds.

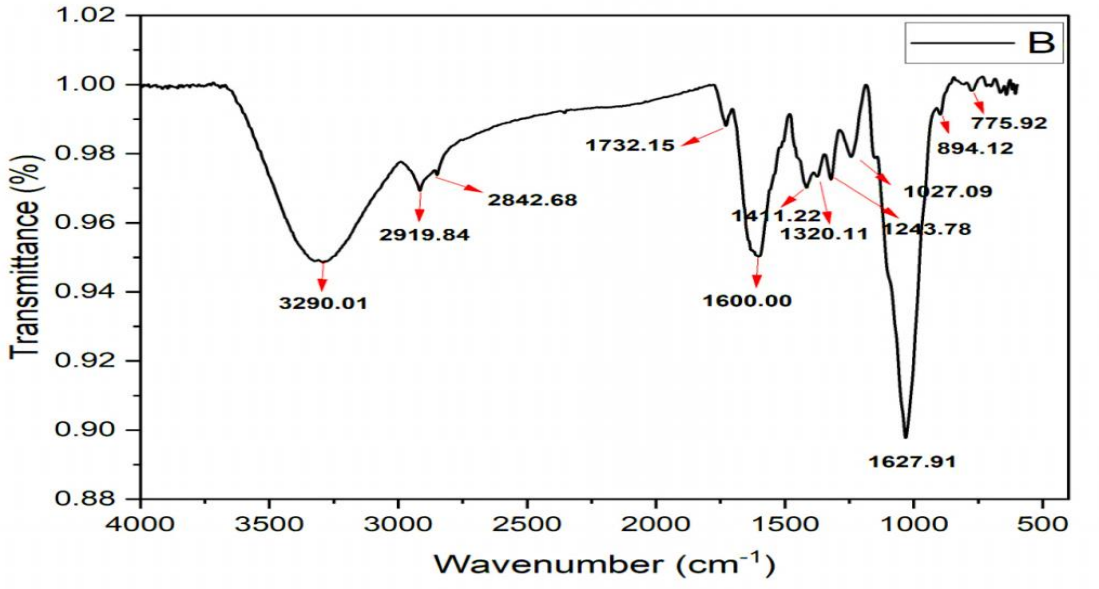


Figure 2. Positions of the FT-IR absorption bands of the extract (4000-500 cm^{-1}).

Table 2. FT-IR band assignments.

Wavenumber (cm^{-1})	Vibration	Functional group / meaning
3290.01	O-H stretch	Hydroxyl (alcohol, phenol)
2919.84	C-H asymmetric stretch	Aliphatic CH_2/CH_3
2842.68	C-H symmetric stretch	Aliphatic CH_2/CH_3
1732.15	C=O stretch	Carbonyl (ester, lactone)
1627.91	C=C stretch	Conjugated alkene / aromatic
1600.00	C=C stretch	Aromatic ring
1411.22	C-H bend	Aliphatic

1320.11	C-O stretch	Phenol / ether
1243.78	C-O-C stretch	Ether / glycosidic linkage
1027.09	C-O stretch	Alcohol / glycoside
894.12	C-H out-of-plane bend	Aromatic substitution pattern
775.92	C-H out-of-plane bend	Aromatic substitution pattern

Fifteen peaks were recorded between 13.9 and 40.2 min (retention time, RT) and corresponded to nine tentatively assigned compounds (Table 3; Figure 3-5). Peaks sharing a name were summed, because several identical library hits at adjacent retention times are expected for isomers, co-eluting species or spectral mis-assignment. The butanedioate ester assignment had the largest combined area among the retained assignments (peaks 5, 7, 9, 11 and 15; 31.78% combined; largest single peak of this compound 12.09% at 39.543 min), followed by two N, N-diethylbenzamide peaks (14.03%), N-(tert-butyl)-2-benzoylbenzamide (13.21%) and dimethyl 2-hydroxy-4-[(tetrahydropyran-2-yloxy) methyl] benzene-1,3-dicarboxylate (8.31%). Area percentage reflects relative peak area, not concentration. All retained assignments eluted within a narrow window near the end of the run (39.1-40.2 min), and the blank chromatogram is not shown, so a contribution from column bleed or carry-over cannot be excluded.

Table 3. Tentative NIST library assignments of GC-MS peaks in the ethanolic leaf extract (peaks with the same assignment summed).

Peak(s)	RT (min)	Compound	Area %	Status
5, 7, 9, 11, 15	39.107-40.195	Butanedioic acid, 2-ethyl-2-(phenylthio)-, 1-ethyl ester	3.06, 12.09, 4.21, 7.49, 4.93 (Σ 31.78)	Tentative assignment
6, 13	39.399, 40.100	N,N-Diethyl-2-(N-phenylamino)-6-methylbenzamide	5.53, 8.50 (Σ 14.03)	Tentative assignment
10, 14	39.797, 40.145	N-(tert-butyl)-2-benzoylbenzamide	9.63, 3.58 (Σ 13.21)	Tentative assignment
8	39.675	Dimethyl 2-hydroxy-4-[(tetrahydropyran-2-yloxy) methyl] benzene-1,3-dicarboxylate	8.31	Tentative assignment
12	40.023	Methyl 3-methyl-5-oxo-2-phenoxyhexanedithioate	4.53	Tentative assignment
1	13.878	Cyclohexasiloxane, dodecamethyl-	12.89	Probable artefact (siloxane bleed)
2	17.487	1,3-Diphenyl-1-[(trimethylsilyl)oxy]-1-heptene	7.82	Probable artefact (silyl derivative)
3	20.722	Tri-O-trimethylsilyl, N-pentafluoropropionyl derivative of terbutaline	4.53	Probable artefact (derivative)
4	23.516	Phosphonous dibromide, [2,2,2-trifluoro-1-(trifluoromethyl)-1-(trimethylsilyloxy)ethyl]-	2.90	Probable artefact (synthetic reagent)

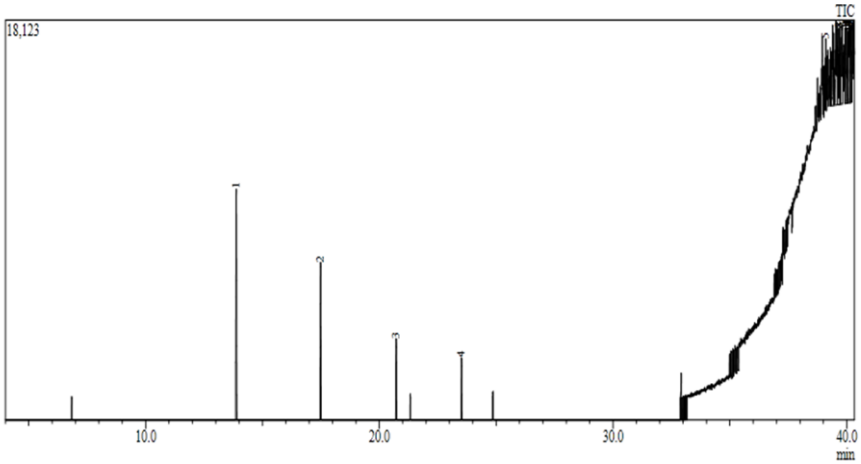


Figure 3. GC-MS total ion chromatogram of the ethanolic leaf extract of *A. paniculata* (peaks numbered as in Table 3).

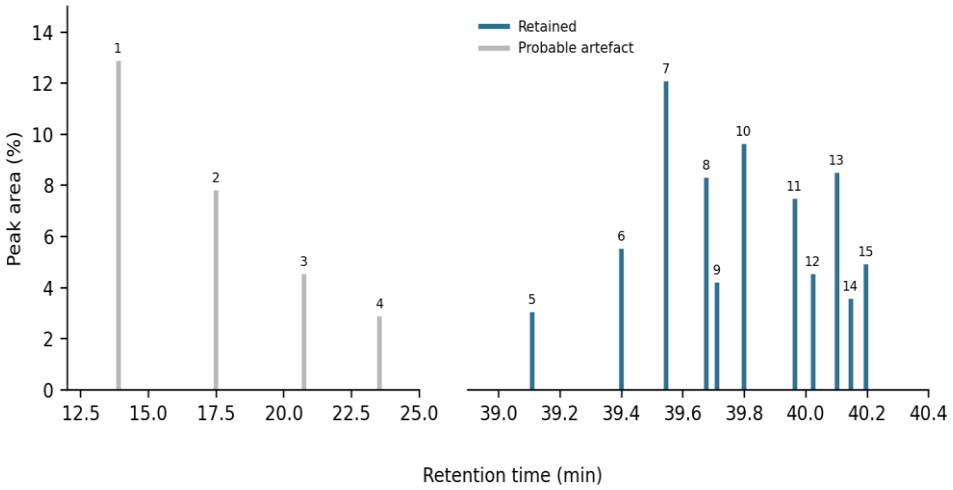


Figure 4. Peak area (%) against retention time for the 15 GC-MS peaks. Grey, probable artefacts; blue, retained peaks.

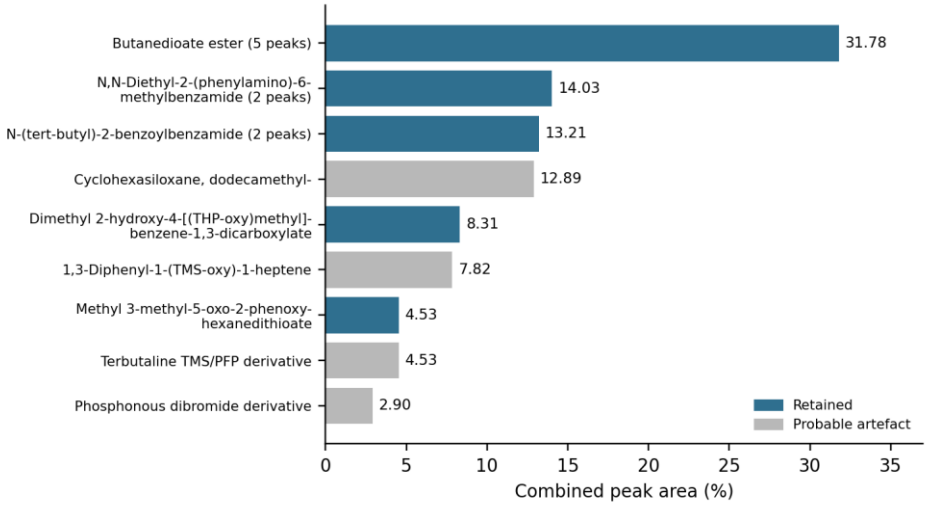


Figure 5. Combined peak area (%) of each tentatively assigned GC-MS compound. Grey bars indicate probable artefacts.

Siloxanes and silylated, fluorinated or brominated reagent-type species are not recognized plant metabolites and are commonly contributed by column bleed, septa or derivatization reagents. They are therefore not interpreted as bioactive constituents of *A. paniculata*. The remaining compounds are aromatic esters and amides of uncertain origin; their natural occurrence in this species is not established, so these assignments are tentative and must be confirmed with authentic standards, and contamination or artefact formation cannot be excluded. The diterpenoid lactones for which the plant is best known (andrographolide and analogues) are polar, thermally labile and poorly volatile, and are normally measured by HPLC or LC-MS rather than underivatized GC-MS. The GC-MS profile reported here therefore describes only the volatile and semi-volatile fraction, and LC-MS/HPLC against reference standards is recommended. Two tentatively assigned compounds were docked: the assignment with the largest combined peak area (butanedioate ester, hereafter Ligand A) and N-(tert-butyl)-2-benzoylbenzamide (Ligand B, $C_{18}H_{19}NO_2$). Ligand B showed lower (more favourable) binding energies than Ligand A for both proteins (Table 4, Figure 6).

Table 4. Exploratory docking results (AutoDock; protocol not validated; binding energy in kcal/mol).

Ligand	Protein	Binding energy	Interacting residues	Interaction types
A	1U7F	−5.54	Arg292, Leu540, Ala546, Met543	2 conventional H-bonds; π-alkyl; alkyl

A	6FX4	−5.40	Thr69, Lys14, Leu67, Arg66, Arg89	2 conventional H-bonds; π-alkyl; carbon H-bond
B	1U7F	−8.05	Glu246, Pro263, Phe248, His249, Leu273	2 conventional H-bonds; π-alkyl; π-cation; π-sigma
B	6FX4	−7.73	Arg89, Lys11, Lys14, Arg12, Arg66, Thr69, Phe87	H-bond; π-cation; alkyl; π-alkyl; π-donor H-bond; π-π stacking

Ligand A, butanedioic acid, 2-ethyl-2-(phenylthio)-, 1-ethyl ester; Ligand B, N-(tert-butyl)-2-benzoylbenzamide.

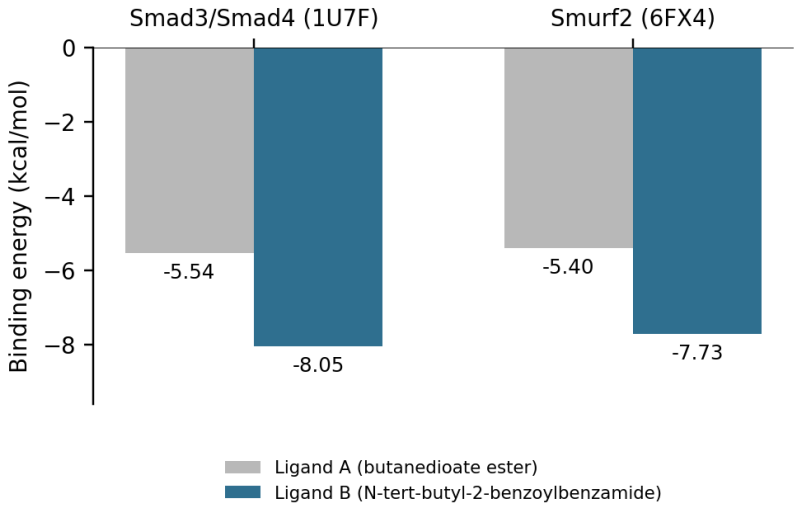
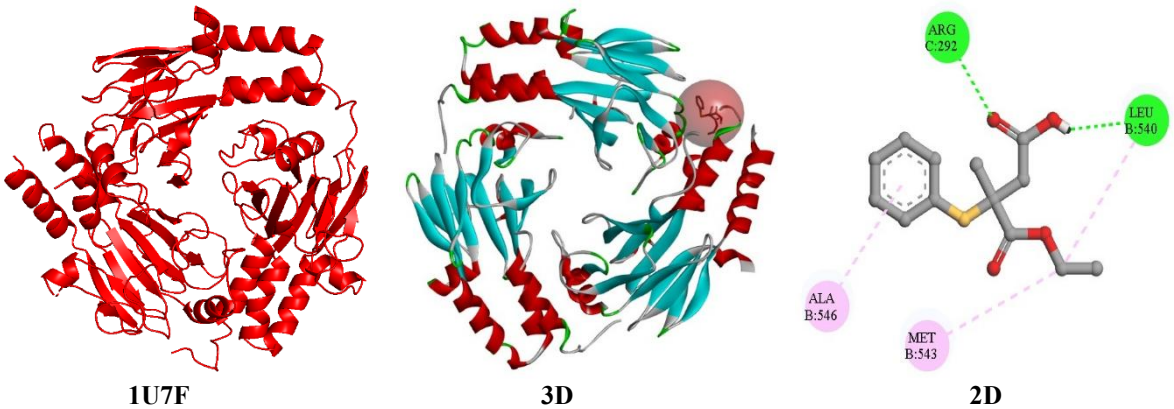


Figure 6. Predicted binding energies (kcal/mol; more negative = stronger predicted binding) of Ligands A and B against Smad3/Smad4 (PDB 1U7F) and Smurf2 (PDB 6FX4).

Ligand B formed hydrogen bonds with Glu246 and Pro263 and aromatic contacts with Phe248, His249 and Leu273 in 1U7F, and an H-bond with Arg89, π-π stacking with Phe87 and π-cation or π-alkyl contacts with Lys11, Lys14, Arg12 and Arg66 in 6FX4 (Figure 7). Ligand A interacted mainly through two H-bonds and non-polar alkyl contacts, which are weaker and less directional. Stronger predicted affinity for Ligand B is therefore consistent with its richer interaction network. This is a hypothesis, not evidence of inhibition: AutoDock energies are approximate estimates, the docking protocol was not validated (no redocking of a reference ligand is reported), no molecular dynamics (MD) simulation was run to test pose stability, and the functional relevance of the docked binding site on each protein has not been established. Notably, the compound with the largest combined peak area (Ligand A) scored less favourably, both assignments are tentative, and the activity of either compound is untested.



1U7F **3D** **2D**

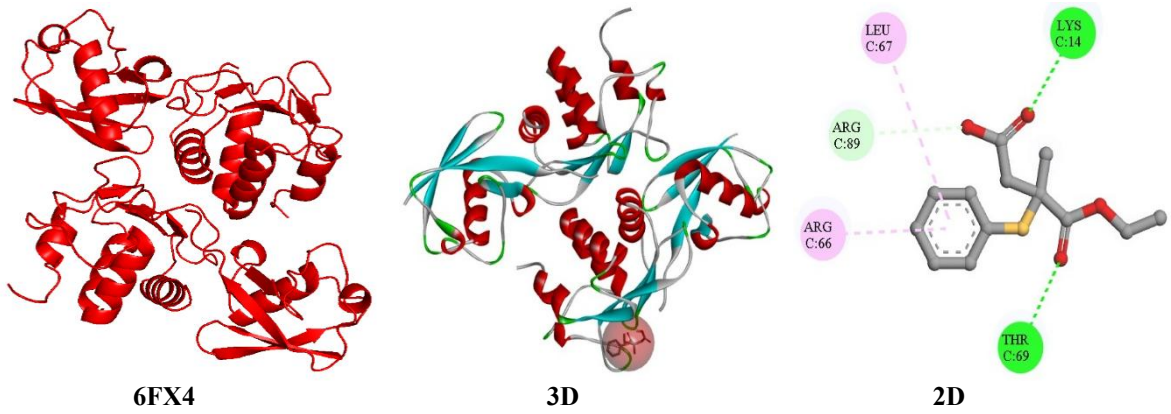


Figure 7. Native protein structures (PyMOL) with 3D and 2D BIOVIA Discovery Studio views of Ligand A and Ligand B docked to 1U7F and 6FX4.

The targets are biologically relevant: 1U7F is the Smad3/Smad4 complex central to TGF-β signalling, and Smurf2 controls Smad turnover (Lin *et al*., 2000; Mekky *et al*., 2025). Natural products have been reported to modulate Smad3 phosphorylation and Smurf2 activity (Zheng *et al*., 2025; Xi *et al*., 2025), which could justify experimental testing of Ligand B (for example, by enzyme or cell-based assays) once its identity has been confirmed. These docking data do not support claims about any specific disease, because no cytotoxicity or cell-line assay was performed. Scavenging was higher at 500 µg/mL than at 100 µg/mL in all three assays (Table 5; Figure 8). At the highest concentration tested, scavenging was 79.13% for DPPH, 72.02% for ABTS and 76.75% for hydroxyl radical, versus 21.32%, 17.32% and 17.28% respectively at the lowest. Only these two concentrations are reported, which is insufficient to define a concentration-response relationship; IC_{50} values were therefore not calculated, and no potency comparison with the ascorbic acid reference can be made. Activity is consistent with the phenols and flavonoids detected, which donate hydrogen atoms or electrons to convert radicals to stable products (Chaudhary *et al*., 2023; Shakil Ahmed *et al*., 2025), but no total phenol or flavonoid content was measured, so a correlation cannot be claimed.

Table 5. Radical scavenging activity (%) of the ethanolic extract at the lowest and highest concentrations tested (single measurements; replicate statistics not available).

Assay	100 µg/mL	500 µg/mL
DPPH	21.32	79.13
ABTS	17.32	72.02
Hydroxyl radical	17.28	76.75

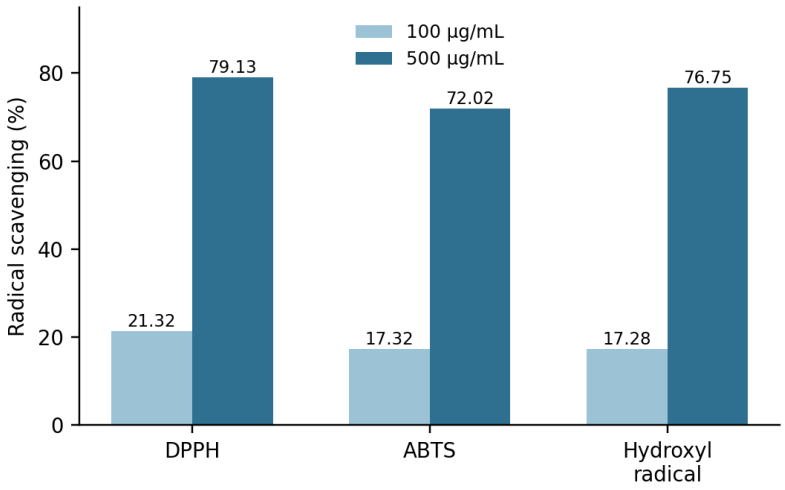


Figure 8. Radical scavenging activity of the extract at 100 and 500 µg/mL in the DPPH, ABTS and hydroxyl radical assays.

The extract produced zones of inhibition against all six organisms, with larger zones at higher volumes for five of the six (Table 6, Figure 9). At 60 µL the largest zones were for *P. aeruginosa* (24 mm), *S. typhimurium* (22 mm) and *C. albicans* (21 mm), followed by *E. coli* (18 mm), *M. luteus* (17 mm) and *C. glabrata* (14 mm) (Figure 10). *C. glabrata* was an exception: its zone fell from 17 mm (40 µL) to 14 mm (60 µL), the cause of which was not investigated (limited diffusion at the higher load and measurement variability are possible explanations, but the data do not distinguish between them). Zone diameter is a qualitative measure of susceptibility, not potency, and the minimum inhibitory concentration (MIC, the lowest concentration that prevents visible growth) was not determined. Zones for the positive controls (amoxicillin for the bacteria, fluconazole for the yeasts) are given in Table 6. The result for the DMSO negative control is not tabulated, and the recorded positive-control zones of 0 mm are not consistent with zone diameters being measured including the 8 mm well. No statistical comparison with the controls was performed. These organisms are clinically relevant: *P. aeruginosa* causes pneumonia and wound and bloodstream infections in immunocompromised patients, and *S. typhimurium* causes gastroenteritis that can become invasive in vulnerable groups (Anju *et al*., 2023; Salman *et al*., 2025). The study did not use drug-resistant isolates, so no claim about activity against antimicrobial-resistant strains is made.

Table 6. Zone of inhibition (mm, including the 8 mm well; single measurements) of the ethanolic extract and of the positive controls (amoxicillin, bacteria; fluconazole, yeasts).

Organism	20 µL	40 µL	60 µL	Positive control
Micrococcus luteus	12	15	17	15
Escherichia coli	13	16	18	14
Pseudomonas aeruginosa	16	22	24	0
Salmonella typhimurium	12	15	22	26
Candida albicans	15	18	21	12
Candida glabrata	12	17	14	0

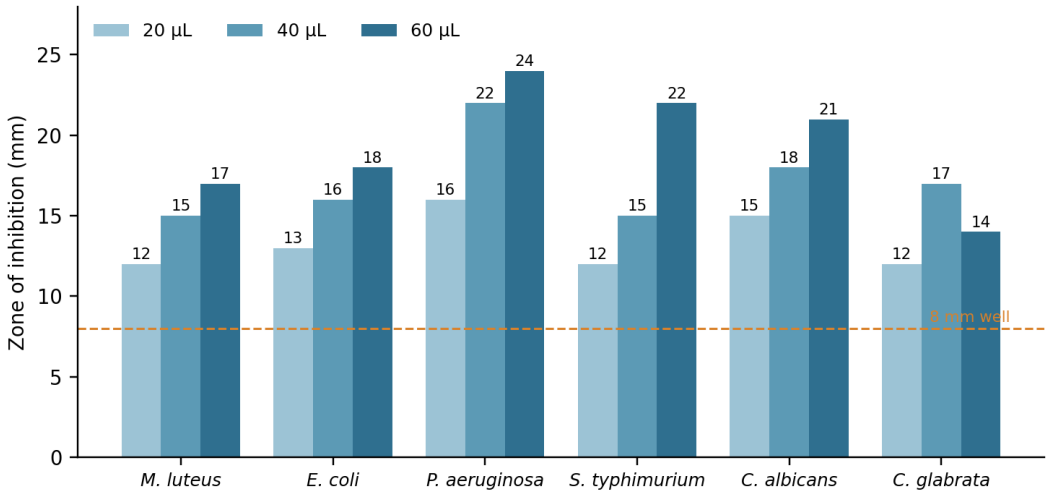


Figure 9. Dose-dependent zones of inhibition against four bacteria and two *Candida* species. The dashed line marks the 8 mm well diameter.

The GC-MS data cover only volatile and semi-volatile compounds and included probable artefacts; the characteristic diterpenoids were not analysed. Compound assignments are tentative library matches that were not confirmed with authentic standards, and the blank chromatogram is not presented. Docking was exploratory; the protocol was not validated by redocking, and the poses were not tested by MD simulation or experiment. Antimicrobial testing was qualitative (no MIC/MBC) and used a single extract, and cytotoxicity and selectivity were not evaluated, so safety and therapeutic relevance are unknown. Antioxidant activity was reported at only two concentrations, so IC_{50} values could not be derived; replicate data and standard deviations are not available for any assay, no inferential statistics were applied, and the raw data were not available for re-analysis.

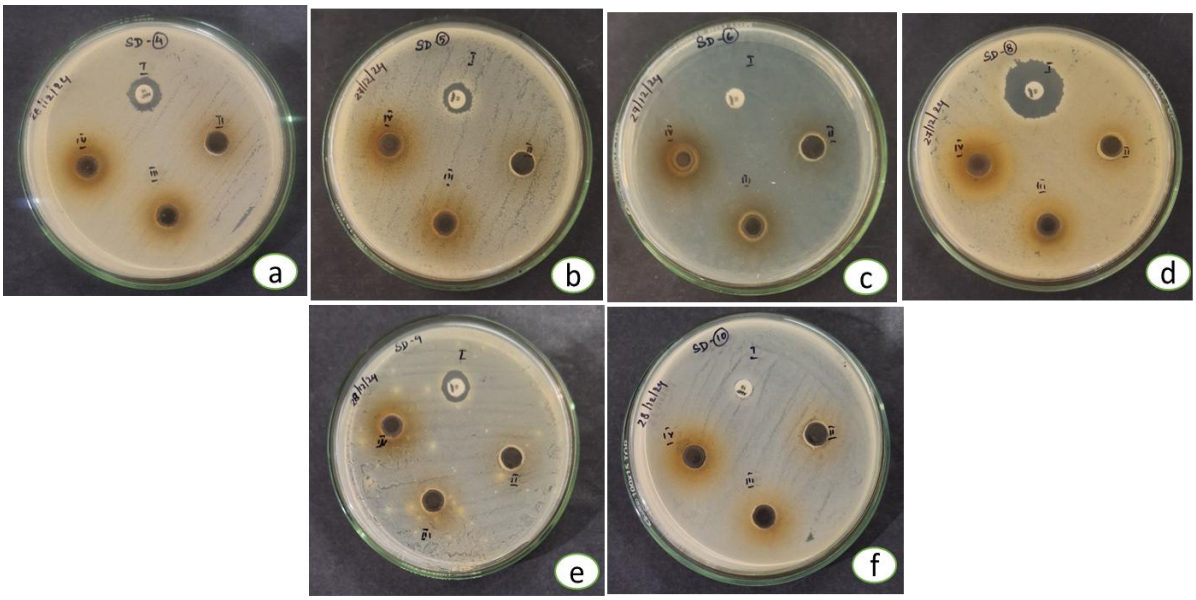


Figure 10. Agar well diffusion plates showing inhibition zones of the extract against (a) *Micrococcus luteus*, (b) *Escherichia coli*, (c) *Pseudomonas aeruginosa*, (d) *Salmonella typhimurium*, (e) *Candida albicans* and (f) *Candida glabrata*.

CONCLUSION

The ethanolic leaf extract of *Andrographis paniculata* contained phenols, flavonoids, tannins, alkaloids, saponins, steroids and terpenoids, showed higher free-radical scavenging at 500 than at 100 µg/mL (79.13% DPPH, 72.02% ABTS and 76.75% hydroxyl radical at 500 µg/mL) and produced inhibition zones against four bacteria and two *Candida* species, the largest zones at 60 µL being for *P. aeruginosa*, *S. typhimurium* and *C. albicans*. In silico, N-(tert-butyl)-2-benzoylbenzamide showed more favourable predicted binding to Smad3/Smad4 and Smurf2 than the tentatively assigned butanedioate ester, which had the largest combined GC-MS peak area. These findings are preliminary, the GC-MS assignments are tentative and the docking results are exploratory; they support further work: replicated assays with full concentration-response data (including IC_{50} determination), LC-MS or HPLC profiling with authentic standards, MIC/MBC determination including resistant isolates, cytotoxicity testing, and validated docking with MD simulation.

ACKNOWLEDGEMENT

The authors thank their institutions for providing the facilities needed to complete this work.

CONFLICT OF INTERESTS

The authors declare no conflict of interest

ETHICS APPROVAL

Not applicable

FUNDING

This study received no specific funding from public, commercial, or not-for-profit funding agencies.

AI TOOL DECLARATION

The authors declare that no AI and related tools are used to write the scientific content of this manuscript.

DATA AVAILABILITY

Data will be available on request

REFERENCES

Anju, V. T., Busi, S., Mohan, M. S., & Dyavaiah, M. (2023). Bacterial infections: Types and pathophysiology. In *Antibiotics - Therapeutic Spectrum and Limitations* (pp. 21-38). Academic Press.

Ansari, P., Reberio, A. D., Ansari, N. J., Kumar, S., Khan, J. T., Chowdhury, S., & Seidel, V. (2025). Therapeutic potential of medicinal plants and their phytoconstituents in diabetes, cancer, infections, cardiovascular diseases, inflammation and gastrointestinal disorders. *Biomedicines, 13*(2), 454.

Arjun, P. (2011). *Investigations on micropropagation and isolation of active compounds from Tribulus terrestris Linn* (Doctoral dissertation, University of Madras, Chennai, India).

Arjun, P., Semwal, D. K., Semwal, R. B., Malaisamy, M., Sivaraj, C., & Vijayakumar, S. (2017). Total phenolic content, volatile constituents and antioxidative effect of Coriandrum sativum, Murraya koenigii and Mentha arvensis. *The Natural Products Journal, 7*(1), 65-74.

Azhagu Madhavan, S., & Arjun, P. (2025). Antihyperglycemic activity of polyphenolic metabolites and biosynthesized silver nanoparticles from Pedalium murex: Characterization and application of antioxidant and uropathogenic antimicrobial activities. *Microbial Pathogenesis, 205*, 107620.

Azhagu Madhavan, S., Arjun, P., Kedari, G. S. R., & Vinay Kumar. (2025). Identification of bio-active compounds and biochemical characterization of green synthesized silver nanoparticles (AgNPs) against selected uropathogenic antimicrobial activity. *Journal of Inorganic and Organometallic Polymers and Materials, 35*(4), 2904-2920.

Azhagu Madhavan, S., Arjun, P., Senthilkumar, S., Yuvaraj, M. F., Nivetha, R., Rajajeyakumar, M., & Ganesan, S. (2024). Biochemical characterization and green synthesis of silver nanoparticles (AgNPs) from Costus spicatus for potential anti-diabetic target in streptozocin (STZ) induced diabetic rats. *Journal of Inorganic and Organometallic Polymers and Materials, 34*(12), 6039-6055.

Balouiri, M., Sadiki, M., & Ibnsouda, S. K. (2016). Methods for in vitro evaluating antimicrobial activity: A review. *Journal of Pharmaceutical Analysis, 6*(2), 71-79.

Brand-Williams, W., Cuvelier, M. E., & Berset, C. (1995). Use of a free radical method to evaluate antioxidant activity. *LWT - Food Science and Technology, 28*(1), 25-30.

Chaudhary, P., Janmeda, P., Docea, A. O., Yeskaliyeva, B., Abdull Razis, A. F., Modu, B., & Sharifi-Rad, J. (2023). Oxidative stress, free radicals and antioxidants: Potential crosstalk in the pathophysiology of human diseases. *Frontiers in Chemistry, 11*, 1158198.

Chen, X., Ren, J., Yang, J., Zhu, Z., Chen, R., & Zhang, L. (2023). A critical review of Andrographis paniculata. *Medicinal Plant Biology, 2*(1).

DeLano, W. L. (2002). PyMOL: An open-source molecular graphics tool. *CCP4 Newsletter on Protein Crystallography, 40*(1), 82-92.

Güler, Ş., Torul, D., Kurt-Bayrakdar, S., Tayyarcan, E. K., Çamsarı, Ç., & Boyacı, İ. H. (2023). Evaluation of antibacterial efficacy of Lawsonia inermis Linn (henna) on periodontal pathogens using agar well diffusion and broth microdilution methods: An in-vitro study. *BioMedicine, 13*(3), 25.

Halliwell, B., Gutteridge, J. M. C., & Aruoma, O. I. (1987). The deoxyribose method: A simple "test-tube" assay for determination of rate constants for reactions of hydroxyl radicals. *Analytical Biochemistry, 165*(1), 215-219.

Hariprasath, L., Jegadeesh, R., Arjun, P., Kumaresan, K., Raaman, N., Vikineswary, S., & Murali, N. (2016). Aqueous extract of Senecio candicans DC induce liver and kidney damage in a sub-chronic oral toxicity study in Wistar rats. *Regulatory Toxicology and Pharmacology, 79*, 25-34.

Lin, X., Liang, M., & Feng, X. H. (2000). Smurf2 is a ubiquitin E3 ligase mediating proteasome-dependent degradation of Smad2 in transforming growth factor-β signaling. *Journal of Biological Chemistry, 275*(47), 36818-36822.

Maria, M. F. F., Ikhmal, W. M. K. W. M., Sabri, M. G. M., Ibrahim, M. S. C., & Adnan, A. (2018). Identification of functional group present in Andrographis paniculata (kalmegh) leaves by FTIR analysis. *IOP Conference Series: Materials Science and Engineering, 440*, 012035.

Mekky, R. H., Abo-El Fetoh, M. E., Faheem, S. A., Radwan, A. F., Fawzy, M. H., Mustafa, A. M., ... Cho, W. C. (2025). Transforming growth factor-β pathway: Biological functions and therapeutic targets. *MedComm, 6*(7), e70278.

Morris, G. M., Huey, R., Lindstrom, W., Sanner, M. F., Belew, R. K., Goodsell, D. S., & Olson, A. J. (2009). AutoDock4 and AutoDockTools4: Automated docking with selective receptor flexibility. *Journal of Computational Chemistry, 30*(16), 2785-2791.

Rahman, S., & Husen, A. (2023). Role of green chiretta [Andrographis paniculata (Burm. f.) Nees] in diabetes and other ailments.

Rana, N., Gupta, P., Singh, H., & Nagarajan, K. (2024). Role of bioactive compounds, novel drug delivery systems, and polyherbal formulations in the management of rheumatoid arthritis. *Combinatorial Chemistry & High Throughput Screening, 27*(3), 353-385.

Re, R., Pellegrini, N., Proteggente, A., Pannala, A., Yang, M., & Rice-Evans, C. (1999). Antioxidant activity applying an improved ABTS radical cation decolorization assay. *Free Radical Biology and Medicine, 26*(9-10), 1231-1237.

Salman, A. S., Yahya, Z. M., & Flaifel, D. K. (2025). Septicemia (blood poisoning). *GSJ, 13*(4).

Shakil Ahmed, Md., Hasan, Md. T., Ahmmed, R., Bismillah, Md., Rahman, M. M., Hossain, M. I., ... Islam, M. A. (2025). Evaluation of methanolic extracts from five important medicinal plants: Phytochemical profiling, antioxidant capacity, in vitro antidiabetic activity, and cytotoxicity assay. *South African Journal of Botany, 184*, 1001-1009.

Sharma, S., Sharma, A., & Gupta, U. (2021). Molecular docking studies on the anti-fungal activity of Allium

sativum (garlic) against mucormycosis (black fungus) by BIOVIA Discovery Studio Visualizer 21.1.0.0. *Annals of Antivirals and Antiretrovirals*. https://doi.org/10.17352/aaa.000013

Sukirtha, R., Suguna, K., Bharathiraja, C., Karthikeyan, K., Arjun, P., Kumar, C., Mysoon, M. A. A., Vimal, S., & Srinivasan, P. (2025). Luminescent biogenic selenium nanoparticles from Indigofera aspalathoides Vahl ex DC: A novel hepatoprotective strategy for enhancing liver health. *Luminescence, 40*, e70101.

Sumathy, R., Azhagu Madhavan, S., Arjun, P., & Pankaj Kumar, C. (2024). Nanomaterial (AgNPs) synthesis using Calotropis gigantea extract, characterization and biological application in antioxidant and antibacterial activity. *Journal of Inorganic and Organometallic Polymers and Materials, 34*(9), 4005-4021.

Sumathy, R., Renuga Devi, N., Alagendran, S., Subramani, C., Sukirtha, R., Dixit, S., Mythili, R., Bharathiraja, C., Arjun, P., & Govindarajan, R. K. (2025). Exploring the nanoparticle fabrication ability of Amaranthus spinosus and its biological functions. *Luminescence, 40*, e70231.

Thai, Q. K., Huynh, P., Tran, T. T., Nguyen, B. H., & Nguyen, H. T. T. (2025). Investigating Andrographis paniculata compounds for apoptosis induction in cancer. *Asian Pacific Journal of Cancer Prevention, 26*(7), 2657.

Valgimigli, L. (2023). Lipid peroxidation and antioxidant protection. *Biomolecules, 13*(9), 1291.

World Health Organization. (2009). *WHO monographs on selected medicinal plants* (Vol. 4). Geneva, Switzerland: Author.

Xi, Y., Zeng, S., Tan, X., & Deng, X. (2025). Curcumin inhibits the activity of ubiquitin ligase Smurf2 to promote NLRP3-dependent pyroptosis in non-small cell lung cancer cells. *International Journal of Oncology, 66*(3), 21.

Zheng, X., Wang, L., Cheng, Y., Lin, H., Liu, S., Chen, X., & Xiang, Z. (2025). Rhein alleviates renal interstitial fibrosis by inhibiting Smad3 phosphorylation in TGF-β/Smad signalling pathway. *Chinese Herbal Medicines*.

© **The Author(s) 2026.** This article is published by the *International Journal of Zoology and Applied Biosciences (IJZAB)* under the terms of the **Creative Commons Attribution 4.0 International License (CC BY 4.0)**. This license permits anyone to share, copy, redistribute, adapt, remix, transform, and build upon the material in any medium or format, provided that appropriate credit is given to the original author(s), the source, and the license, and that any changes made are indicated.